Journal of Applied Physics

Facile fabrication of highly ordered poly(vinylidene fluoride-trifluoroethylene) nanodot arrays for organic ferroelectric memory

Cite as: J. Appl. Phys. **119**, 014104 (2016); https://doi.org/10.1063/1.4939601
Submitted: 29 September 2015 . Accepted: 23 December 2015 . Published Online: 06 January 2016

Huajing Fang, Qingfeng Yan, Chong Geng, Ngai Yui Chan, Kit Au, Jianjun Yao, Sheung Mei Ng, Chi Wah Leung, Qiang Li, Dong Guo, Helen Lai Wa Chan, and Jiyan Dai

Facile fabrication of highly ordered poly(vinylidene fluoride-trifluoroethylene) nanodot arrays for organic ferroelectric memory

Huajing Fang,[1,2] Qingfeng Yan,[2,a)] Chong Geng,[2] Ngai Yui Chan,[1] Kit Au,[1] Jianjun Yao,[3] Sheung Mei Ng,[1] Chi Wah Leung,[1] Qiang Li,[2] Dong Guo,[4] Helen Lai Wa Chan,[1] and Jiyan Dai[1,a)]

[1]*Department of Applied Physics, The Hong Kong Polytechnic University (PolyU) Hunghom, Kowloon, Hong Kong*
[2]*Department of Chemistry, Tsinghua University, Beijing 100084, China*
[3]*Asylum Research, Oxford Instruments, Shanghai 200233, China*
[4]*Institute of Acoustics, Chinese Academy of Sciences, Beijing 100190, China*

(Received 29 September 2015; accepted 23 December 2015; published online 6 January 2016)

Nano-patterned ferroelectric materials have attracted significant attention as the presence of two or more thermodynamically equivalent switchable polarization states can be employed in many applications such as non-volatile memory. In this work, a simple and effective approach for fabrication of highly ordered poly(vinylidene fluoride–trifluoroethylene) P(VDF-TrFE) nanodot arrays is demonstrated. By using a soft polydimethylsiloxane mold, we successfully transferred the 2D array pattern from the initial monolayer of colloidal polystyrene nanospheres to the imprinted P(VDF-TrFE) films via nanoimprinting. The existence of a preferred orientation of the copolymer chain after nanoimprinting was confirmed by Fourier transform infrared spectra. Local polarization switching behavior was measured by piezoresponse force microscopy, and each nanodot showed well-formed hysteresis curve and butterfly loop with a coercive field of ~62.5 MV/m. To illustrate the potential application of these ordered P(VDF-TrFE) nanodot arrays, the writing and reading process as non-volatile memory was demonstrated at a relatively low voltage. As such, our results offer a facile and promising route to produce arrays of ferroelectric polymer nanodots with improved piezoelectric functionality. © *2016 AIP Publishing LLC*.
[http://dx.doi.org/10.1063/1.4939601]

I. INTRODUCTION

As the requirements grow for modern electronic products, organic materials are playing more and more important role in many aspects owing to their solution processability, low processing temperature, lightweight, and high flexibility. Ferroelectric polymers, in particular, the polyvinylidene fluoride (PVDF) and its copolymers with trifluoroethylene (TrFE), have received intensive interests due to their useful dielectric, ferroelectric, pyroelectric, and piezoelectric properties.[1–6] One of the emerging research topics about ferroelectric P(VDF-TrFE) copolymer is to scale down its size to nanometer dimension, which may offer unique characteristics and extend its applications ranging from nanosensors to non-volatile memory and nanogenerators.[7–9] The fabrication of two-dimensional (2D) ferroelectric nanodot arrays is an ideal approach for forming isolated nanodomains. Each nanodomain can be treated as an individual functional cell possessor with bistable dipole polarizations, which can be repeatedly switched upon application of an external electric field.

Different techniques have been applied successfully to pattern ferroelectric material into 2D nanodot array, including focused ion beam milling,[10] dip-pen lithography,[11] electron beam direct writing,[12] templating,[13] and nanoimprint lithography (NIL).[14] Among these nanofabrication techniques, NIL has gained considerable attention due to the low power consumption, cost reduction, short fabrication time, and the ability for mass production. Efforts have been made by several research groups to fabricate patterns by NIL, where ferroelectric polymer film is pressed against a pre-patterned hard mold. However, fabrication of these hard imprint molds is usually expensive and complicated because it involves technique such as electron beam lithography[15] and anodic oxidation.[16]

Self-assembly of colloidal spheres has been demonstrated to be a high-throughput and inexpensive strategy for surface patterning.[17–19] By using a self-assembled monolayer colloidal crystal as a template, a number of methods have been developed to fabricate well-ordered 2D periodic arrays of micro- and nanostructures such as rings, bowls, cones, and columns.[20–23] Herein, we report a facile and reproducible method to prepare regular array of ferroelectric polymer nanodots with the combination of self-assembly of polystyrene (PS) spheres and nanoimprinting. By using a soft polydimethylsiloxane (PDMS) mold, we have successfully transferred the 2D array pattern from the initial colloidal monolayer to the imprinted P(VDF-TrFE) films over a large area. Compared to the hard mold method as reported before,[15,16] this soft PDMS mold generates conformal contact of spherical confinement with the target surface and greatly reduces the imprint pressure. The PDMS mold can be

[a)]Authors to whom correspondence should be addressed. Electronic addresses: yanqf@mail.tsinghua.edu.cn and jiyan.dai@polyu.edu.hk

used with a number of times without special treatments for reworking between imprints. Moreover, the period of the nanodots can be easily manipulated based on the large tunability of PS spheres size.[24,25] Therefore, the approach offers a promising route for patterning 2D array on a wide range of organic functional materials. In addition, we have demonstrated the potential application of these ordered P(VDF-TrFE) nanodot arrays as non-volatile memory with a relatively low operation voltage.

II. EXPERIMENTAL

A. Preparation of P(VDF-TrFE) thin film

The P(VDF-TrFE) copolymer with 70/30 mol. % was supplied by Piezotech, France and used as-received. The copolymer powder was dissolved in methyl ethyl ketone (MEK) at a concentration of 2 wt. %. After filtering through a 0.22 μm pore-size polytetrafluoroethylene (PTFE) filter, the solution was then spin-coated (3000 rpm for 30 s) on a commercial Pt/Ti/SiO_2/Si substrate (200 nm/50 nm/500 nm/500 μm, Hefei Kejing Material Technology Co., Ltd.). All procedures were carried out at room temperature. The film thickness of about 200 nm has been obtained and confirmed by atomic force microscope (AFM, Veeco Nanoscope V).

B. Fabrication of P(VDF-TrFE) nanodot arrays

Experimental procedures for the fabrication of ferroelectric nanodots array are schematized in Fig. 1. Glass slide piece was treated with freshly prepared piranha solution (H_2SO_4 and H_2O_2 in 3:1 volume ratio) for 20 min to render the surface hydrophilic. Monodisperse PS colloidal spheres of 440 nm in diameter with a polydispersity less than 3% were synthesized using the emulsifier-free emulsion polymerization method.[24] The PS nanosphere monolayer was prepared first on a cleaned glass substrate by using the air/water interface self-assembly process as stated in our earlier works.[26,27] Briefly, 10–20 μl PS spheres water/ethanol suspension were dropped on the water surface along the inside wall of a glass Petri dish ($\Phi = 8$ cm). The PS spheres spread freely onto the water surface and assembled into 2D arrays immediately once the suspension contacted the water. To consolidate this colloidal array into a large-area monolayer, a drop of 1 wt. % sodium dodecyl sulfate (SDS) solution which could reduce the water surface tension was added. The floating PS colloidal monolayer was carefully transferred to the cleaned glass slide. Second, the PDMS prepolymer was casted on the PS nanospheres monolayer and treated under vacuum to remove the entrained air bubbles. Then, the PDMS prepolymer was cured at 70 °C for 5 h in an oven. The solidified PDMS was peeled off from the PS spheres template and used as a nanoimprinting mold. To facilitate the peeling off process after imprinting, the as prepared PDMS mold was coated with a trichloromethylsilane (TMCS) vapor for anti-adhesion. Thermal imprinting was carried out at 170 °C and 0.35 bars for 10 min using a house-built parallel plate imprint tool. The temperature of the NIL processing was well above the melting point of P(VDF-TrFE) so that the molten polymer with a low viscosity could completely fill the nanocavities in the printing mold under such a low pressure. The pressure was held until the system was cooled to room temperature at a rate of 10 °C/min. Then, the PDMS mold was carefully peeled off from the patterned film. The ferroelectric polymer nanodots array was obtained and used without any other cumbersome treatments.

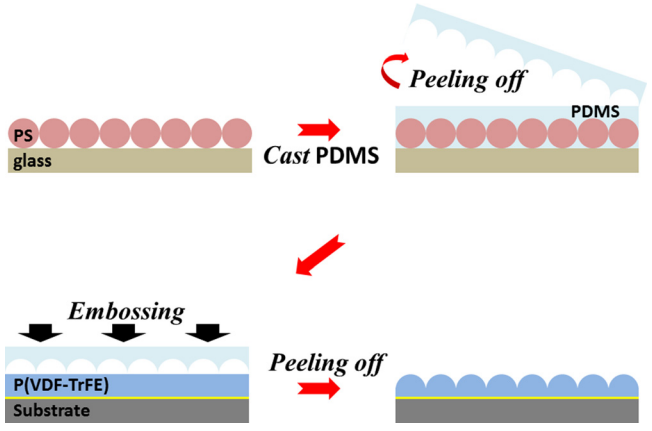

FIG. 1. Schematic diagram of the fabrication process for ferroelectric P(VDF-TrFE) nanodots array.

C. Characterization

Field emission scanning electron microscope (FESEM, JEOL JSM-6335F) was used to examine the surface morphology of PS spheres, PDMS mold, the continuous P(VDF-TrFE) thin films, and the nano-imprinted P(VDF-TrFE) thin films. The crystal structures of the P(VDF-TrFE) film and nanodot array were characterized through X-ray diffraction (XRD, Rigaku SmartLab). Fourier transform infrared (FTIR) spectra were obtained under reflection mode by a Nicolet 380 FTIR spectroscopy. The surface of the P(VDF-TrFE) nanodot array was imaged in tapping mode with an atomic force microscopy (AFM, Veeco Nanoscope V). To study the local piezoresponse and ferroelectric effect of the annealed P(VDF-TrFE) film and nanodots array, the samples were examined by piezoresponse force microscopy (Cypher PFM, Asylum Research, Oxford Instruments, Santa Barbara) for surface topographies. The PFM tip (Asyelec AC240, spring constant 2 N/m) with Ti/Pt coating was used.

III. RESULTS AND DISCUSSION

The self-assembled PS spheres were hexagonally close-packed in a large-area monolayer, as revealed in Fig. 2(a), where the inset shows the details of these PS spheres with a diameter of ~420 nm. As shown in Fig. 2(b), the PDMS mold obtained by casting the prepolymer against PS spheres shows the patterned hemispherical holes in a hexagonal close-packed lattice. Figs. 2(c) and 2(d) are the SEM images of the annealed P(VDF-TrFE) thin film and imprinted nanodots arrays, respectively. Randomly oriented needle-like grains can be observed on the surface of the continuous thin film, indicating the semi-crystalline structure. For the imprinted P(VDF-TrFE) nanodots, homogeneous pattern with the same lamellae structure can be observed in a long

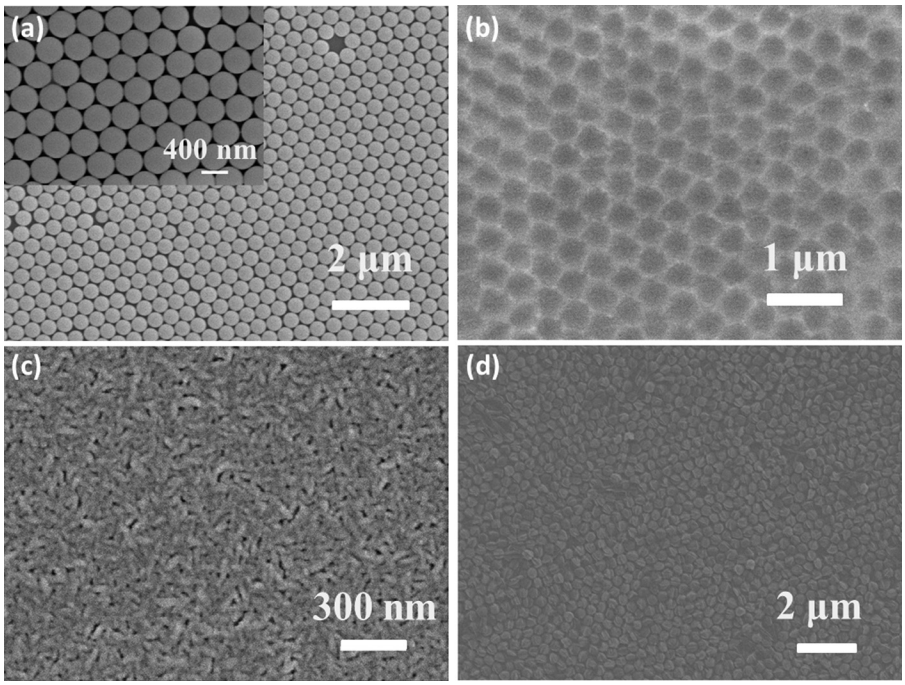

FIG. 2. SEM images of (a) PS nanospheres monolayer, the inset shows a magnified image of the PS nanospheres, (b) the PDMS mold, (c) the annealed P(VDF-TrFE) continuous thin film, and (d) large-scale ferroelectric P(VDF-TrFE) nanodots array fabricated by nano-imprinting.

range periodicity. Since the lateral size of the confinement posed by the PDMS molds is well above the average lamellar length in continuous films, the crystal nucleation in the nanodots was not severely affected.

The crystalline phase, localized chain conformation, and orientation of the nanoimprinted thin film were characterized by FTIR. For a better comparison, the solution-derived continuous thin film after annealing at 120 °C was also characterized. Fig. 3(a) shows the FTIR spectra of the nanoimprinted and continuous P(VDF-TrFE) thin film. The absorption peaks near 850, 887, and 1293 cm^{-1} in the spectra of continuous thin films indicate the presence of the desirable ferroelectric β-phase.[28] Moreover, the band near 1293 cm^{-1} has been assigned to the symmetric CF_2 stretching vibration, coupled with the backbone stretching and bending. It has a transition dipole moment $\boldsymbol{\mu_b}$ parallel to the polar $\boldsymbol{b}$ axis. Compared to the continuous thin film, this band shows a significant reduction in the nanoimprinted thin film, meaning that the $\boldsymbol{b}$ axis is strongly titled away from the substrate. The band at 1403 cm^{-1} belongs to the CH_2 wagging vibration with the dipole moment $\boldsymbol{\mu_c}$ along the chain direction $\boldsymbol{c}$ axis. The absorption band at 1193 cm^{-1} can be assigned to the antisymmetric stretching and rocking vibration of CF_2 with the dipole moment $\boldsymbol{\mu_a}$ parallel to the $\boldsymbol{a}$ axis. These two bands are more prominent in the nanoimprinted thin film, indicating the in-plane orientation of the $\boldsymbol{a}$ and $\boldsymbol{c}$ axes.[29] A high $\boldsymbol{b}$ axis orientation of the ferroelectric polymer parallel to the direction of the applied electric field is the determining factor for successful device performance. Such preferential orientation is advantageous due to the optimum of the effective electric field perpendicular to the substrate,[30] as will be shown shortly. It should be pointed out that the imprinting temperature (170 °C) was higher than that used in recent studies (approximately 100 °C and 150 °C).[15,29] At this temperature, the molten P(VDF-TrFE) showed a low viscosity and could easily fill in the mold with a low pressure 0.35 bars used in this work, which was much lower than that reported previously (60 bars).[15,29] Also, the previously reported nanoimprinting process required advanced equipment rather than our house-built parallel plate imprint tool. Moreover, it is

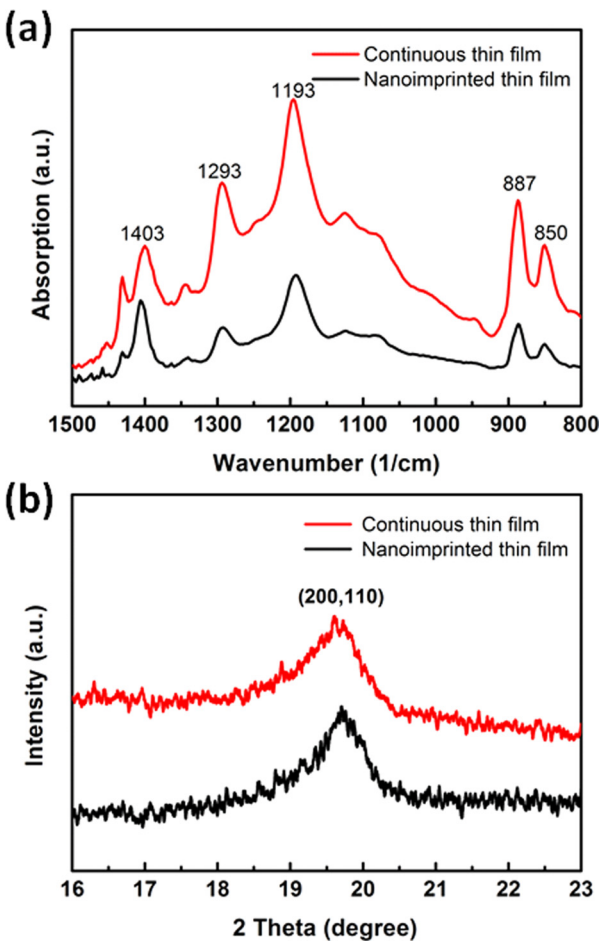

FIG. 3. (a) FTIR spectra and (b) XRD pattern of the annealed continuous thin film (red line) and nanoimprinted thin film (black line).

very difficult to imprint the liquid crystalline hexagonal phase with PDMS mold, as PDMS itself is not hard enough.

We also confirmed the ferroelectric β-phase of these samples by XRD. As shown in Fig. 3(b), the prominent diffraction peak at around $2\theta = 19.8^\circ$ corresponds to the (200) and (110) diffractions of the ferroelectric β-phase of P(VDF-TrFE)[28] and can be seen in both the nanoimprinted and the continuous thin films. This result indicates that our nanoimprint process upon the melting point does not affect the crystalline phase of the polymer adversely. One notable issue in the NIL processes in making P(VDF-TrFE) nanodots array is that the imprinting temperature determines the quality of pattern which influence the functional properties of the imprinted film. The abrupt and irreversible reduction of polarization in crystallized P(VDF-TrFE) upon melting and recrystallization always restricts the thermal treatments that control the crystalline orientations during the nanoimprint process.[31] To avoid recrystallization, the amorphous film after spin-coating was nanoimprinted directly without the annealing process in this work. The rapid thermal processing well above the melting point to the amorphous P(VDF-TrFE) does not affect the crystalline quality of the polymer, even when heated up to 250 °C.[32,33]

Fig. 4 displays the AFM images of the nanoimprinted thin film, where the 3D and topography images of the obtained nanoimprint thin film show a hexagonal hemispherical dots array with very few defects. It should be noted that the nanodots consist of the randomly oriented lamellae rather than a smooth spherical surface. Along the A-B direction, the nanodots arranged with a period of 437 nm. This value is consistent with the average diameter of PS nanospheres. The line profile along the corner to corner direction (A-C) shows interesting features involving two structures. The big features have the size of 500 nm in width and 172 nm in height. The small features, 280 nm in width and 54 nm in height, are observed at the interparticle edges between two neighbouring hemispheres. Thus, the nanodots appear to be oblate hemispheres with heights less than one third of their diameters. Such kind of morphology evolution has been observed previously in nanoimprinting hemisphere microlens arrays by using PDMS soft mold.[25] The morphology of the nanodots actually inherited from the PDMS mold, which had an inverted oblate hemisphere shape as shown in Fig. 2(b). The discrepancy of shape between the PDMS mold and the original PS sphere shown in Fig. 2(a) resulted mainly from additional thermal deformation of PS nanospheres during the PDMS curing step. Furthermore, the elastic behavior of PDMS mold might also exacerbate the formation of oblate hemispheres during the subsequent nanoimprinting step.[25] Nanoimprint process normally results in a residual layer. The thickness of the original P(VDF-TrFE) film spin-coated on the substrate was 200 nm. As shown in Fig. 4, the height of nanodots along the A-B direction was ~130 nm, thus a residual layer of at least 70 nm in thickness was expected for the nanodot arrays attained.

To confirm the ferroelectricity and piezoresponse of the P(VDF-TrFE) thin film after imprinting, the local domain switching behavior of nanodots was measured by PFM incorporated with a lock-in technique. A small AC voltage (1 V) with a frequency of 290 kHz was applied to the sample via a PFM tip without a top electrode. Characteristic hysteresis loop as shown in Fig. 5(a) reveals the existence of a switchable intrinsic polarization in P(VDF-TrFE) nanodots. The apparent coercive field (E_c) acquired at the center of nanodot is ~62.5 MV/m, which is comparable to previous work.[16] The nanoimprinted thin film also exhibits a well-shaped butterfly loop in the piezoelectric amplitude signal. The continuous P(VDF-TrFE) thin film as a control was also investigated (shown in Fig. 5(b)), and the coercive field of a 200 nm thick film is about 75 MV/m, which is larger than the bulk

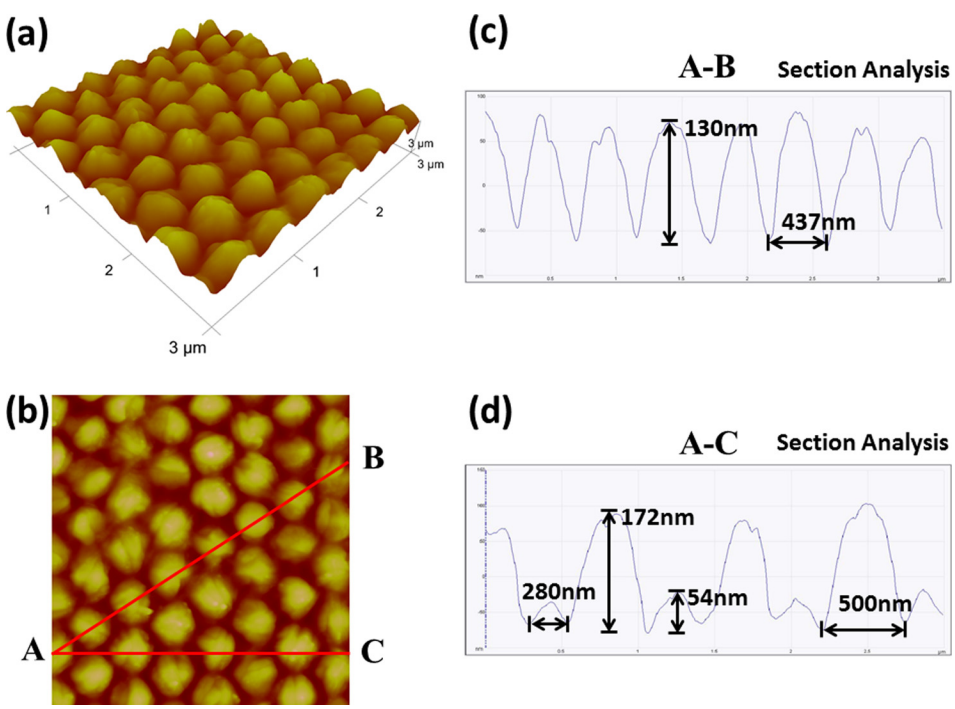

FIG. 4. AFM data of P(VDF-TrFE) nanodots array fabricated by nanoimprinting. (a) A typical 3D image, (b) 2D image, and (c) and (d) the line profile along A-B and A-C, respectively.

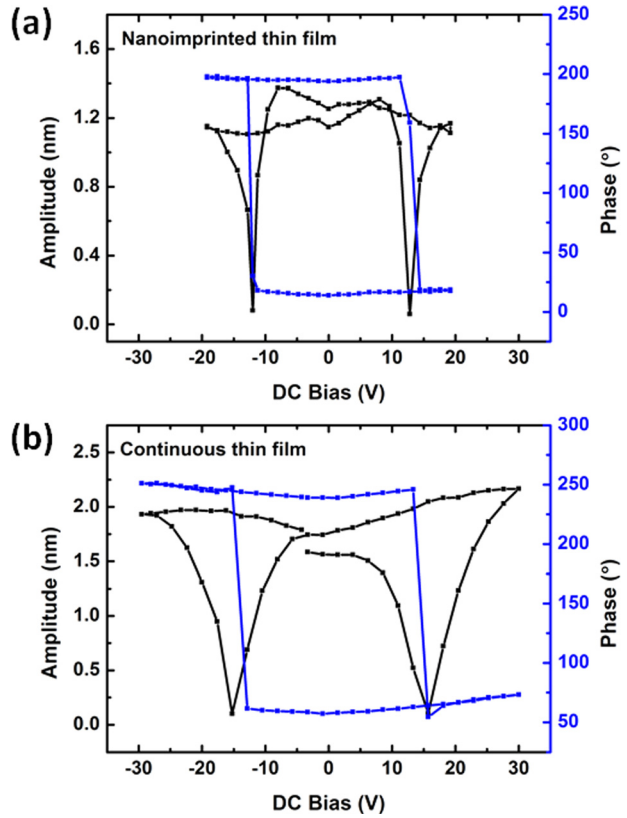

FIG. 5. The piezoresponse amplitude butterfly loop (black curve) and the phase loop (blue curve) of P(VDF-TrFE) of (a) a nanoimprinted thin film and (b) a continuous thin film.

counterparts (50 MV/m). Such a divergence in coercive field is often observed in ferroelectric thin films, which may be caused by the different switching field distribution between the microscopic PFM and conventional ferroelectric tests.[34,35] Compared to the continuous thin film, nanodots usually have relatively lower coercive field due to the preferential orientation of copolymer chain and the less entanglement with adjacent nanodots.[16,36]

The ferroelectric polymer with a regular pattern enables a number of applications such as high-performance non-volatile memory devices for data storage, since the application of a small DC voltage between the conductive tip and bottom Pt electrode generates an electric field which is high enough to induce 180° polarization switching in each nanodot, while the upward or downward polarization state can be denoted as Boolean 1 or 0 that forms a well-established binary memory system.[37] The writing process on the imprinted nanodot array was demonstrated in our imprinted P(VDF-TrFE) nanodots array. The tip was scanned on the nanodots over a 5 μm × 5 μm area and three nanodots were poled with 20 V DC bias to form the designed triangular pattern. This written information can be subsequently read out by monitoring the piezoelectric vibration of the same area under AC voltage. Figs. 6(a) and 6(b) show the PFM amplitude and phase images of the imprinted P(VDF-TrFE) nanodots array after writing the triangular pattern, respectively. In the piezoelectric amplitude image (Fig. 6(a)), represented by color scale bar in nanometers, local polarization domains with different brightness are shown. The distinct bright and dark contrasts clearly highlight the ferroelectric property in the individual P(VDF-TrFE) nanodot. The PFM image in Fig. 6(a) indicates that the three tip-poled nanodots have much lower PFM amplitude than the surrounding unpoled nanodots. Furthermore, the area surrounding the tip-poled dots shows higher PFM amplitude than in their centers. These anomalies in PFM amplitude difference might be ascribed to the artifact caused by the cross-talk between piezoresponse and topography, as observed by Kalinin *et al.*[38,39] Phase image in Fig. 6(b) displays an excellent correlation with the amplitude

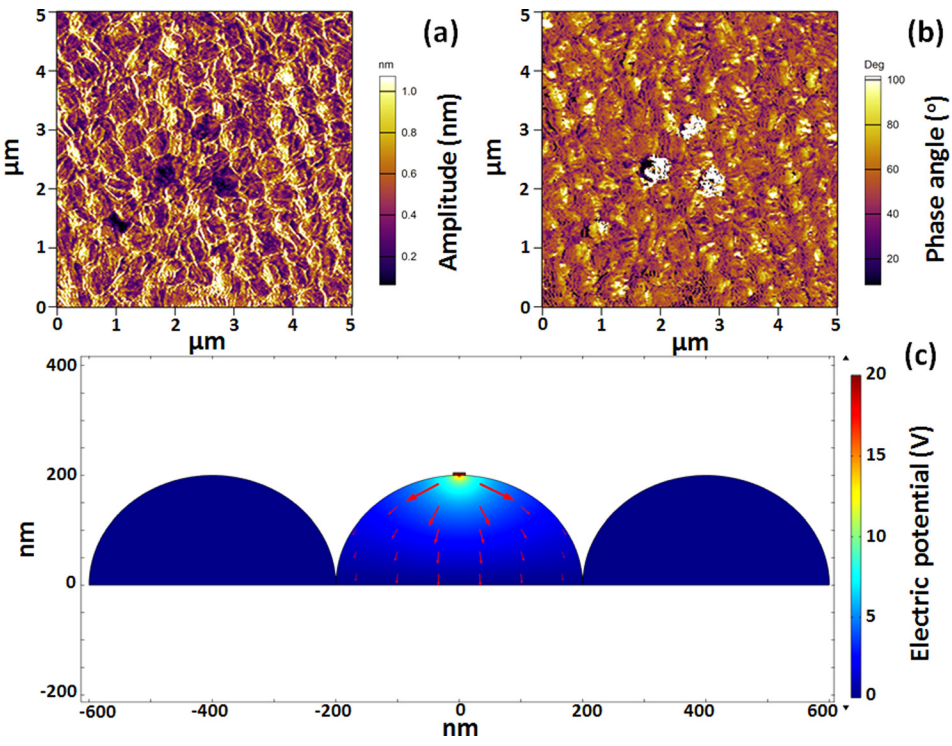

FIG. 6. PFM images showing (a) amplitude and (b) phase profile of P(VDF-TrFE) nanodots array fabricated by nano-imprinting, as a demonstration of data memory. (c) The electric field distribution simulation with PFM tip located at the top of the nanodot.

result, where the triangular pattern consists of three cells appearing as bright area with phase angle that different from the unwritten area. More importantly, the switching appears to be rather uniform, without any cross-talk between adjacent cells. It is also noted that these written patterns recorded on the ferroelectric polymer can be erased by applying the reverse voltage and rewritten with a different distribution of positive or negative voltage during scanning.

In order to study the electric field distribution through the P(VDF-TrFE) nanodot with a very localized top electrode, finite element modelling via Comsol Multiphysics was performed. As shown in Fig. 6(c), the top disk represents the PFM tip. To simplify the finite element modelling, we have ignored some features such as the tip shape and the nanomorphology of the crystallites within the nanodots.[40] After applying a DC voltage of 20 V between the conductive tip and bottom electrode, large electric field can be observed across the P(VDF-TrFE) nanodot. The field direction is indicated by the red arrows, while the field strength is proportional to the size of the arrows. It is clear that the resulting electric field underneath the PFM tip is not uniform, the field strength of the region away from the tip decreased significantly. Note that the field strength distributed in the adjacent nanodots is almost zero. Hence, the ferroelectric switching of P(VDF-TrFE) is limited to a single cell. These simulation results suggest that the spatial extent of the field produced by the PFM tip is finite and the isolated nanodots can effectively prevent the cross talk of each cell, which agrees well to the PFM amplitude and phase images.

IV. CONCLUSION

In summary, we have demonstrated a method to transfer the 2D array pattern from the colloidal monolayer to ferroelectric P(VDF-TrFE) copolymer film by using soft PDMS as the nanoimprint lithography mold. This soft PDMS mold generates a conformal contact so that imprinting can be realized at a very low pressure. XRD and FTIR results proved the desirable ferroelectric β-phase with a preferential orientation of the imprinted nanodots. Excellent ferroelectricity of the imprinted nanodots has been confirmed by PFM. Based on the local domain switching behavior, the patterned ferroelectric P(VDF-TrFE) nanodot array can be used in a wide range of applications such as non-volatile memory cells for data storage. The isolated nanodots can effectively prevent the cross talk of each cell comparing to the continuous film. Finally, combining colloidal self-assembly and nanoimprint is an effective approach to pattern high-quality and high-density 2D array in other functional materials applied to organic devices.

ACKNOWLEDGMENTS

This research was supported by the National key Basic Research Program of China (973 Program) under Grant No. 2013CB632900, The Hong Kong Polytechnic University strategic projects (Nos. 1-ZVCG and 1-ZE25), and the National Science Foundation of China (Nos. 51173097 and 91333109). The Tsinghua University Initiative Scientific Research Program (No. 20131089202), the Tsinghua National Laboratory for Information Science and Technology (TNList) Cross-discipline Foundation, and the Open Research Fund Program of the State Key Laboratory of Low-Dimensional Quantum Physics, Tsinghua University (No. KF201516) are also acknowledged for partial financial support.

[1]B. Chu, X. Zhou, K. Ren, B. Neese, M. Lin, Q. Wang, F. Bauer, and Q. M. Zhang, Science **313**, 334 (2006).
[2]Z. Lü, T. Pu, Y. Huang, X. Meng, and H. Xu, Nanotechnology **26**, 055202 (2015).
[3]S. S. Fu, H. Yu, J. H. Hu, S. J. Ding, Q. Cheng, Y. L. Jiang, and G. D. Zhu, J. Appl. Phys. **113**, 114102 (2013).
[4]J. F. Scott, Science **315**, 954 (2007).
[5]A. Baji, Y. W. Mai, Q. Li, and Y. Liu, Nanoscale **3**, 3068 (2011).
[6]A. Laudari and S. Guha, J. Appl. Phys. **117**, 105501 (2015).
[7]L. Persano, C. Dagdeviren, Y. Su, Y. Zhang, S. Girardo, D. Pisignano, Y. Huang, and J. A. Rogers, Nat. Commun. **4**, 1633 (2013).
[8]Y. L. Sun, D. Xie, J. L. Xu, T. T. Feng, Y. Y. Zang, C. Zhang, R. X. Dai, X. J. Meng, and Z. Y. Ji, J. Appl. Phys. **118**, 115501 (2015).
[9]N. Soin, T. H. Shah, S. C. Anand, J. Geng, W. Pornwannachai, P. Mandal, D. Reid, S. Sharma, R. L. Hadimani, D. V. Bayramol, and E. Siores, Energy Environ. Sci. **7**, 1670 (2014).
[10]M. Hambe, S. Wicks, J. M. Gregg, and V. Nagarajan, Nanotechnology **19**, 175302 (2008).
[11]J. Y. Son, Y. H. Shin, S. Ryu, H. Kim, and H. M. Jang, J. Am. Chem. Soc. **131**, 14676 (2009).
[12]J. H. Ferris, D. B. Li, S. V. Kalinin, and D. A. Bonnell, Appl. Phys. Lett. **84**, 774 (2004).
[13]W. Ma, D. Hesse, and U. Gösele, Small **1**, 837 (2005).
[14]Y. Liu, D. N. Weiss, and J. Li, ACS Nano **4**, 83 (2010).
[15]H. G. Kassa, R. Cai, A. Marrani, B. Nysten, Z. Hu, and A. M. Jonas, Macromolecules **46**, 8569 (2013).
[16]X. Z. Chen, Q. Li, X. Chen, X. Guo, H. X. Ge, Y. Liu, and Q. D. Shen, Adv. Funct. Mater. **23**, 3124 (2013).
[17]T. Wang, X. Li, J. Zhang, Z. Ren, X. Zhang, X. Zhang, D. Zhu, Z. Wang, F. Han, X. Wang, and B. Yang, J. Mater. Chem. **20**, 152 (2010).
[18]Y. H. Jhang, Y. T. Tsai, C. H. Tsai, S. Y. Hsu, T. W. Huang, C. Y. Lu, M. C. Chen, Y. F. Chen, and C. C. Wu, Org. Electron. **13**, 1865 (2012).
[19]Z. Sun, Y. Li, J. Zhang, Y. Li, Z. Zhao, K. Zhang, G. Zhang, J. Guo, and B. Yang, Adv. Funct. Mater. **18**, 4036 (2008).
[20]Z. F. Dai, C. Lee, B. Kim, C. Kwak, J. Yoon, H. Jeong, and J. Lee, ACS Appl. Mater. Interfaces **6**, 16217 (2014).
[21]J. Zhang, Y. Li, X. Zhang, and B. Yang, Adv. Mater. **22**, 4249 (2010).
[22]S. G. Jang, H. K. Yu, D. G. Choi, and S. M. Yang, Chem. Mater. **18**, 6103 (2006).
[23]D. Brodoceanu, R. Elnathan, B. Prieto-Simon, B. Delalat, T. Guinan, E. Kroner, N. Voelcker, and T. Kraus, ACS Appl. Mater. Interfaces **7**, 1160 (2015).
[24]S. Shim, Y. Cha, J. Byun, and S. Choe, J. Appl. Polym. Sci. **71**, 2259 (1999).
[25]H. J. Nam, D. Jung, G. Yi, and H. Choi, Langmuir **22**, 7358 (2006).
[26]C. Geng, L. Zheng, H. Fang, Q. Yan, T. Wei, Z. Hao, X. Wang, and D. Shen, Nanotechnology **24**, 335301 (2013).
[27]C. Geng, L. Zheng, J. Yu, Q. Yan, T. Wei, X. Wang, and D. Shen, J. Mater. Chem. **22**, 22678 (2012).
[28]S. Oh, Y. Kim, Y. Y. Choi, D. Kim, H. Choi, and K. No, Adv. Mater. **24**, 5708 (2012).
[29]Z. Hu, M. Tian, B. Nysten, and A. M. Jonas, Nat. Mater. **8**, 62 (2009).
[30]Y. J. Park, S. J. Kang, C. Park, K. J. Kim, H. S. Lee, M. S. Lee, U. I. Chung, and I. J. Park, Appl. Phys. Lett. **88**, 242908 (2006).
[31]S. J. Kang, Y. J. Park, I. Bae, K. J. Kim, H. C. Kim, S. Bauer, E. L. Thomas, and C. Park, Adv. Funct. Mater. **19**, 2812 (2009).
[32]X. Li, Y. F. Lim, K. Yao, F. E. H. Tay, and K. H. Seah, Phys. Chem. Chem. Phys. **15**, 515 (2013).
[33]J. Y. Son, I. Jung, and Y. Shin, J. Phys. Chem. C **117**, 12890 (2013).
[34]D. Y. Wang, D. M. Lin, K. S. Wong, K. W. Kwok, J. Y. Dai, and H. L. W. Chan, Appl. Phys. Lett. **92**, 222909 (2008).
[35]T. Watanabe, H. Funakubo, M. Osada, H. Uchida, I. Okada, B. J. Rodriguez, and A. Gruverman, Appl. Phys. Lett. **90**, 112914 (2007).
[36]Z. Hu, G. Baralia, V. Bayot, J. F. Gohy, and A. M. Jonas, Nano Lett. **5**, 1738 (2005).

[37]R. C. G. Naber, K. Asadi, P. W. M. Blom, D. M. Leeuw, and B. Boer, Adv. Mater. **22**, 933 (2010).
[38]S. V. Kalinin, S. Jesse, B. J. Rodriguez, J. Shin, A. P. Baddorf, H. N. Lee, A. Borisevich, and S. J. Pennycook, Nanotechnology **17**, 3400 (2006).
[39]S. V. Kalinin, E. Karapetian, and M. Kachanov, Phys. Rev. B **70**, 184101 (2004).
[40]A. Bernal, A. Tselev, S. Kalinin, and N. Bassiri-Gharb, Adv. Mater. **24**, 1160 (2012).